Research Papers
Issue RP0137
July 2012

Impact on Soil and Coast Division (ISC)

Performance evaluation of a regional climate simulation with COSMO-CLM in the Alpine space

By **Myriam Montesarchio**
Impact on Soil and Coast Division (ISC), Euro-Mediterranean Center on Climate Change (CMCC), *m.montesarchio@cira.it*

Maria Paola Manzi
Impact on Soil and Coast Division (ISC), Euro-Mediterranean Center on Climate Change (CMCC), *m.manzi@cira.it*

Luigi Cattaneo
Impact on Soil and Coast Division (ISC), Euro-Mediterranean Center on Climate Change (CMCC), *l.cattaneo@cira.it*

Edoardo Bucchignani
Centro Italiano Ricerche Aerospaziali, CIRA
Impact on Soil and Coast Division (ISC), Euro-Mediterranean Center on Climate Change (CMCC), *e.bucchignani@cira.it*

and **Paola Mercogliano**
Centro Italiano Ricerche Aerospaziali, CIRA
Impact on Soil and Coast Division (ISC), Euro-Mediterranean Center on Climate Change (CMCC), *p.mercogliano@cira.it*

SUMMARY This paper analyzes the capabilities of Limited Area Model COSMO-CLM to simulate the main features of the observed climate over an area characterized by complex terrain. A simulation driven by ERA40 Reanalysis of the XX century climate (1971-2000) has been performed at a spatial resolution of 8 km, in order to provide an assessment of regional model performance on local scale for impact studies. 2-meters temperature (minimum, maximum and average values) and total precipitation have been analyzed, comparing their values with two observational datasets: ETH for precipitation and EOBS for temperature.

1 - INTRODUCTION

The achievement of a finer spatial resolution in the climate simulations is one of the main problems for researchers. High resolution is important because the impacts of climate changes on human society, such as on crops production, wild fires development and hydrogeological risk are related to small scale phenomena [17]. This is especially true for areas whose topography is particularly complex, such as in Alpine region.
The Alps constitute the most relevant topographic ridge of Europe and influence atmospheric circulation on a wide time-spatial scales range. As a consequence of its complex geography, the region exhibits a variety of different climates, ranging from maritime influences (both from the Mediterranean Sea and the Atlantic Ocean) to continental features (such as the plains of Eastern Europe and the inner Alpine valleys) and from low-elevation to mountain climates [4]. The complex topography and land sea distribution of the study area are responsible for numerous mesoscale flow features and precipitation processes in response to synoptic-scale disturbances. Due to limited extension of Alpine catchments, this area represents an interesting benchmark for the investigation of relationship between heavy precipitation and flood events; at the same time, due to coarse grained soil covers, high intensity rainfalls are able to induce rapid and/or extremely rapid shallow landlides. For all these reasons, the Alps constitute an ambitious test ground for regional climate model, but it is also in such regions where the need for climate downscaling is more necessary.
In recent years, therefore, climate modelling community has devoted an increasing interest to Regional Climate Models (RCMs), which have more and more proved to be useful investigation tools on spatial scales not manageable by General Circulation Models (GCM) [2].
Over the years, several approaches have been developed for the use of models suitable for areas characterized by complex topography. In the studies of Faggian and Lionello ([8]), the projections of future climate change provided by 20 Atmospheric-Ocean General Circulation Models (AOGCMs) participating in the Coupled Model Intercomparison Project 3 (CMIP3) were taken, with focus on the Italian region and in particular on the Italian Greater Alpine Region (GAR). They analyzed historical and future simulations of monthly-mean surface air temperature (T) and total precipitation (P) [8]. Im et al. [11], in a recent work, applied a mosaic-type parameterization of subgrid-scale topography over the Alpine region with the regional model RegCM3 by the NCEP reanalysis of observations, employing a spatial resolution of 15 km and land surface subgrid of 3-km resolution. In their successive work [12], they used a surrogate climate change (SSC) simulation with RegCM3 to assess the importance of local controls of regional climate change over the Alps. They obtained significant results, even if the SSC approach does not allow simulating the effects of changes in large-scale circulations. The regional climate model COSMO CLM, adopted in this work, has been widely validated in different projects with the aim to demostrate its ability to serve as a RCM in comparison with other RCMs. Scientists of the BTU Cottbus carried out the major part of this validation and they found the COSMO CLM to be in the same range of accuracy as other RCMs resolving similar scales. In particular, COSMO CLM was successfully applied in the PRUDENCE project [7] exhibiting competitive results [14]. Moreover COSMO-CLM, adopted in the present paper, has been largely used for the understanding of the worldwide climate features in different previous works [13]. The COSMO-CLM configuration adopted by CMCC

in this work (8 km resolution) has been already validated in another work concerning the Mediterranean area [1] exhibiting good results within the comparison of modeled and measured mean 10 meter wind speed and atmospheric pressure at mean sea level values for selected stations in the North Adriatic area. Moreover, using a lower horizontal resolution (14 km) the CMCC's COSMO-CLM configuration has already been validated in the Alpine area [5]. The main reason for the present work is the upgrade of these previous simulations at 14 km, with the aim of analysing the capabilities of the model in simulating the main features of the observed climate using, at this time, an higher resolution, below 10 km. In particular, due to the large use of these data for impact studies and to the scarce availability of adequate datasets for the validation of high resolution climate simulations, the attention is devoted to the validation of the 2 meter temperature and precipitation and their extreme indices. The paper is organized as follows: section 2 is devoted to a short description of model, simulation set-up and observation datasets. In section 3, results related to 2-meters temperature (minimum, maximum and average values) and total precipitation distribution are shown; these results are compared with the observations. Finally, in section 4, a summary of the main results and conclusions is presented.

2 - MODEL AND DATA

2.1 - THE COSMO-CLM MODEL

At CMCC, the regional climate model COSMO-CLM [13] is currently used to perform regional high resolution climate simulations. It is the climate version of the COSMO LM model [16], which is the operational non hydrostatic mesoscale weather forecast model developed initially by the German Weather Service and then by the European Consortium COSMO. Successively, the model has been updated by the CLM Community, in order to develop also a version for climate applications (COSMO-CLM). The development of COSMO-CLM has been driven by two main reasons [14]: the first was the idea of developing a model able to simulate both weather and climate and the second was the need of introducing a non hydrostatic formulation, in order to have a convection resolving weather simulation. This last one is a very important topic, due to the difficulty in predicting the effects of this phenomenon, such as sudden high-intensity rainfall. In particular, on the GAR area, the convection is the main cause of heavy precipitation, due to summertime convection and heavy thunderstorms [6]. COSMO -CLM can be used at a spatial resolution between 1 and 50 km, even if the non hydrostatic formulation of the dynamical equations in LM made it eligible especially for the use at horizontal grid resolution lower than 20 km [3]. At the same time, the use of a higher resolution, with respect to the typical resolution scale of the GCMs, allows describing better the terrain orography and, in particular, the orographic component of precipitation, closely related to the soil morphology. The mathematical formulation of COSMO-CLM is made up of the Navier Stokes equations for a compressible flow. The atmosphere is treated as a multicom-

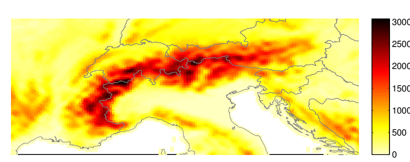

Figure 1:
COSMO CLM domain orography for a configuration with horizontal resolution of 8 km.

ponent fluid (made up of dry air, water vapour, liquid and solid water) for which the perfect gas equation holds. The atmosphere is, moreover, subject to the gravity and to the Coriolis forces. The model includes several parameterizations, in order to keep into account, at least in a statistical manner, several phenomena that take place on unresolved scales, but that have significant effects on the meteorological interest scales (for example, interaction with the orography). The main features of the COSMO-CLM simulation are: nonhydrostatic, full compressible hydrothermodynamical equations in advection form; base state: hydrostatic, at rest. The main prognostic variables are horizontal and vertical Cartesian wind components, pressure perturbation, temperature, specific humidity, cloud water content. Optionally it is also possibile to add the following prognostic variables: cloud ice content, turbulent kinetic energy, specific water content of rain, snow and graupel. About coordinate system, a generalized terrain following height coordinate with rotated geographical coordinates is implemented with user defined grid stretching in the vertical direction (see Figure 2). In order to resolve the

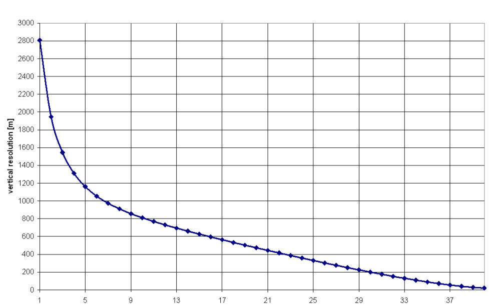

Figure 2:
Vertical grid stretching used for the two set-up configurations: the first level is the highest one while the last level is located at about 20 meters from the ground

near surface turbulent motion, a high vertical resolution is used near surface (20-70m) and a low resolution in the upper atmosphere (500-1500 m). Different options for the definition of vertical levels are available: base state pressure based height coordinate, GalChen height coordinate and exponential height coordinate (SLEVE) according to Schar et al. [15]. The model state variables are staggered using an Arakawa C-grid, Lorenz vertical grid staggering. For the time integration, a time splitting scheme between fast and slow modes is used, with the possibility to adopt a Runge Kutta or Leapfrog time integration scheme. For the spatial discretization, a second-order difference technique is adopted. The parallelization is done by horizontal domain decomposition using a soft-coded gridline halo (2 lines for Leapfrog, 3 for the Runge-Kutta scheme). The Message Passing Interface software (MPI) is used for message passing on distributed memory machines. Details on the model dynamics and physics are available in [16] and in [3].

2.2 - SIMULATION SET-UP

The main features of the simulation set-up are briefly summarized. The COSMO-CLM model version used to run the simulation is 4.8_CLM13 and for the interpolator, INT2LM, the model version is 1.10_CLM2. The simulation has been carried out with boundary conditions provided by the ERA40 Reanalysis, characterized by a horizontal resolution of 1.125° (about 128 km). The horizontal resolution adopted in the simulation, instead, is of 0.0715° (about 8 km). The simulated period is 1971-2000. Concerning the validation, the analysed period is 1972-1998 for the precipitation (availability of ETH dataset) and 1972-2000 for the temperature (availability of EOBS dataset). The first year of the simulation has not been considered to exclude the spin-up period influenced by initial conditions. In Table 1, the main features of the simulation are summarized.

Table 1
Main features of the COSMO-CLM set-up.

Driving data	ERA40
Horizontal resolution	8 km
Num. of Grid points	207 x 211
Num. of vertical levels in the atm.	40
Num. of soil levels	7
Soil scheme	TERRA-ML
Time step	40 s
Melting processes	yes
Convection scheme	TIEDTKE
Frequency of radiation computation	1 hour
Time integration	Runge-Kutta (3rd ord.)
Frequency update boundary cond.	6 hours

2.3 - OBSERVATIONAL DATASET

The model evaluation on daily precipitation was performed by using the "'Alpine Precipitation Analyses from High-Resolution Rain Gauge Observations" [9], here also called ETH. It represents a comprehensive set of mesoscale gridded daily precipitation for the period 1971-1998 with resolution of 0.25° x 0.17° (about 28x20 km). This dataset was created by the Swiss Federal Institute of Technology Zuerich (ETH) and it makes use of a unique dataset of rain gauge observations from the high resolution networks of all Alpine countries. These networks constitute one of the densest meteorological observing systems over complex topography worldwide (Figure 3). The other dataset used for the model evaluation is EOBS: it is an European daily high-resolution (0.25 x 0.25) gridded data set (Figure 4) for precipitation, minimum, maximum, and mean surface temperature and sea level pressure for the period 1950-2010 . This dataset has been designed to provide the best estimate of grid box averages rather than point values to enable direct comparison with RCMs [10].

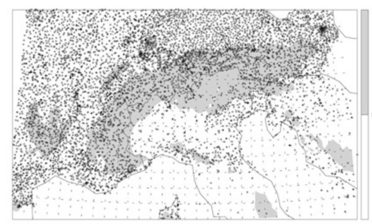

Figure 3:
Station coverage of "'Alpine Precipitation Analyses from High-Resolution RainGauge Observations"'. The distribution of stations is fairly balanced over the northern and western portions of the analysis domain, while the coverage is less dense and less homogeneous for the southern region (northern Italy).

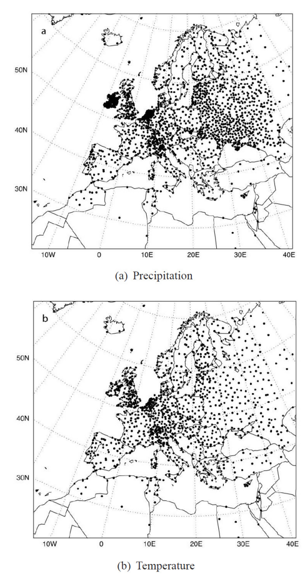

Figure 4:
The complete gridding region, showing the station network for (a) precipitation and (b) temperature of the EOBS dataset.

3 - VALIDATION

The simulation reliability is evaluated considering the values of 2-meters mean, minimum and maximum temperatures and total precipitation. Results related to temperature and precipitation are treated in two different sections as follows: seasonal cycle, trend and mean seasonal values are calculated; then, statistical analyses are performed through pdfs and extremes (the last one using some of the precipitation/temperature indices defined by the World Meteorological Organization (WMO) Expert Team on Climate Change Detection and Indices (ETCCDI,http://cccma.seos.uvic.ca/ETCCDI)). The extreme indices have been obtained with Meteolab (http://www.meteo.unican.es/en/software/meteolab), an open-source Matlab toolbox for statistical (data mining) analysis in meteorology, which allows loading observations and numerical weather and climate models (gridded fields) and performing basic meteorology and climate analysis computations in an easy form.

3.1 - TEMPERATURE

The validation has been performed comparing the temperature with the EOBS dataset.

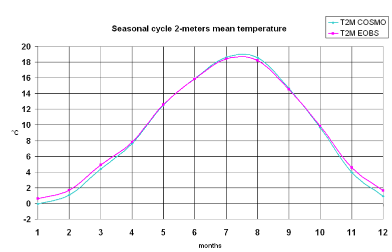

Figure 5:
Seasonal cycle of 2-meters mean temperature of COSMO-CLM (cyan) and EOBS (magent).

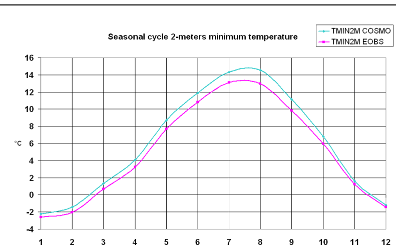

Figure 6:
Seasonal cycle of 2-meters minimum temperature of COSMO-CLM (cyan) and EOBS (magent).

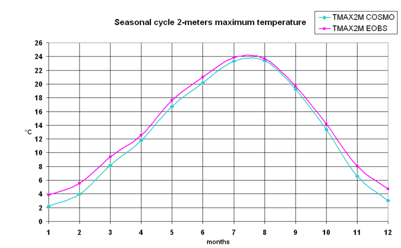

Figure 7:
Seasonal cycle of 2-meters maximum temperature of COSMO-CLM (cyan) and EOBS (magent).

The seasonal cycle (Figures 5 - 7) and the trend (Figures 8 - 10) for mean, maximum and minimum daily temperature (averaged over the whole domain) are very well captured.

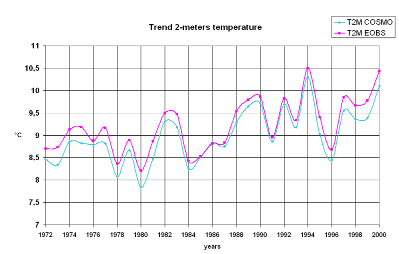

Figure 8:
Trend of 2-meters mean temperature of COSMO-CLM (cyan) and EOBS (magent).

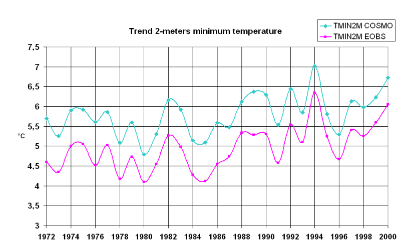

Figure 9:
Trend of 2-meters minimum temperature of COSMO-CLM (cyan) and EOBS (magent).

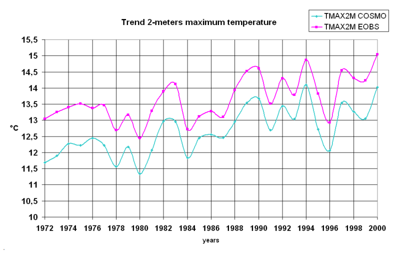

Figure 10:
Trend of 2-meters maximum temperature of COSMO-CLM (cyan) and EOBS (magent).

Regarding mean temperature, there is a general slight underestimation (-0.2°C on average), more marked in the trend in the first years of the simulation but never higher than -0.4°C.

The minimum and maximum temperatures have an opposite bias, both in trend and seasonal cycle: the first one is characterized by an overestimation, while the second is interested by an underestimation. In particular, the mean bias of minimum temperature is 0.8°C, with a peak of almost 1.1°C in the trend and nearly 1.6°C in the month of August in the seasonal cycle (in general, the highest error is in the summer months). Regarding the maximum temperature, a general underestimation of -1°C occurs: in this case, with respect to the minimum temperature, the error is higher from December to March.

Figures 11, 12, 15, 16 show the 2-meters temperature distribution obtained with COSMO-CLM, averaged over the time period 1972-2000, for the four seasons. Figures 13, 14, 17 and 18 show the maps of the related biases, with respect to the EOBS dataset: it's possible to see a general underestimation on the Alps, especially in the winter season when, in the Ligurian Alps, it reaches -3°C, while other regions share a very low bias (between -0.5°C and -1°C). In the summer, a general overestimation occurs on the plains, especially on the Po Valley.

However, in general, differences in absolute value do not exceed 3°C, which is reached on some areas in winter and summer seasons, whereas in spring and autumn the bias is mostly under 1°C.

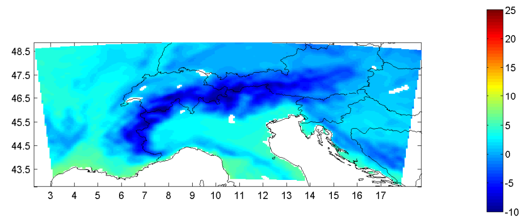

Figure 11:
Winter 2-meters mean temperature (°C), from COSMO-CLM.

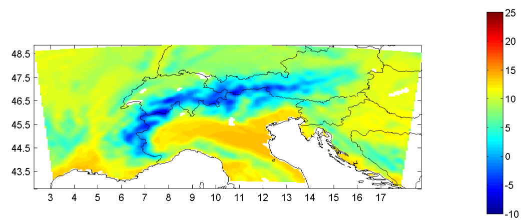

Figure 12:
Spring 2-meters mean temperature (°C), from COSMO-CLM.

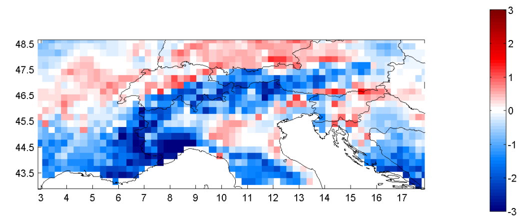

Figure 13:
Bias of winter 2-meters mean temperature (°C) of COSMO-CLM in respect to EOBS data.

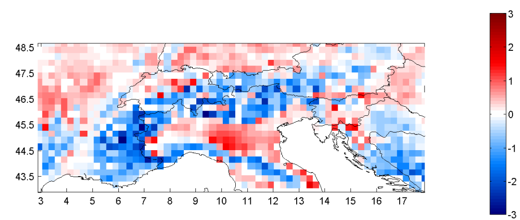

Figure 14:
Bias of spring 2-meters mean temperature (°C) of COSMO-CLM in respect to EOBS data.

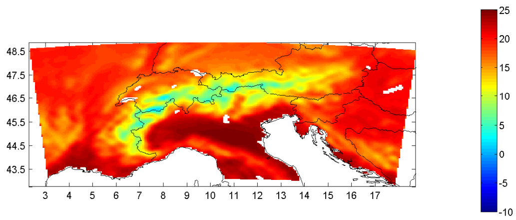

Figure 15:
Summer 2-meters mean temperature (°C), from COSMO-CLM.

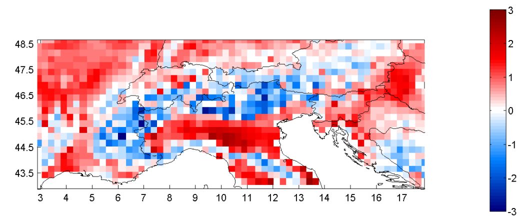

Figure 17:
Bias of summer 2-meters mean temperature (°C) of COSMO-CLM in respect to EOBS data.

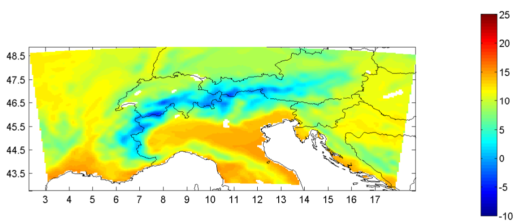

Figure 16:
Autumn 2-meters mean temperature (°C), from COSMO-CLM.

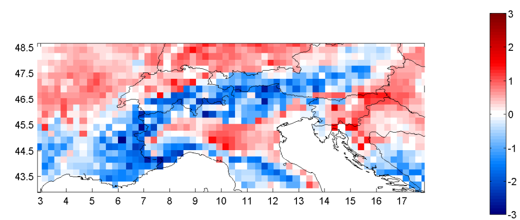

Figure 18:
Bias of autumn 2-meters mean temperature (°C) of COSMO-CLM in respect to EOBS data.

Figures 19, 20 and 21 show the density functions for mean, minimum and maximum daily temperature respectively.
For the first one (Figure 19), a higher probability, with respect to the observations, is associated with the low values of the distribution and the ones higher than 23°C. The two peaks are reached instead at the same values of temperature (about 2-3°C and 15-16°C), both by the regional model COSMO-CLM and the EOBS dataset.
Looking at the minimum temperature, the pdf shows a similar trend; the largest difference is in the values above 15°C, where the regional model attributes a higher probability, such as for minimum temperatures lower than -10°C.
For the maximum temperature, up to 12°C the pdf of COSMO-CLM seems to have a "shift"' to the left; in fact, analyzing the tails of the distribution, the regional model attributes a higher probability, compared to the EOBS dataset, to values lower than 5°C , whereas above 20°C the opposite occurs.
The distribution tails are also represented in the form of temperature percentiles. Figures 22, 23 24 show the 10th percentile distribution for mean, minimum and maximum daily temperature respectively; Figures 25, 26 and 27 the related maps of bias with respect to EOBS data. Similarly, Figures 28, 29 30 show the 90th percentile distribution for mean, minimum and maximum daily temperature respectively; Figures 31, 32 and 33 the related maps of bias with respect to EOBS data. As expected, Alpine areas are much colder than the surrounding, especially compared to the Po Valley, which lies directly underneath and usually shows temperatures of 15°C and higher. Looking at 2-meters mean temperatures provided by the model, values may vary from -12°C (10th) to 5°C (90th) in highest Alpine areas, but they are lower than EOBS dataset: 10th percentiles are downshifted, especially on the areas with a very high orography (Alps and Appennines), while 90th one shows a close match over the Alps and an overestimation on the plains.
Moreover, results about both minimum and maximum daily temperatures are available too. According to simulations, in highest Alpine areas minimum values oscillate between -15°C and 3°C, while maximum are within the range of -10°C/10°C. If compared with EOBS dataset, some differences are evident: on the Alps, the 10th percentile of minimum temperatures is underestimated of 2°, while for maximum there is an average shift of -3°C; for 90th ones, minimum values have a similar trend as the mean temperatures, while maximum shows an underestimation on the northern part of the domain and an overestimation on the south, although the differences do not exceed 2°C in absolute values.
It worth noting to observe that all the areas surrounding Alps often show a completely opposite behaviour: in fact, they are characterized not only by generally warmer temperatures, but also the values estimated by the climate model are higher than observed ones, especially for minimum percentiles. As Alpine areas are significantly higher than the other ones on the map, a suitable conclusion is that model analysis is strongly influenced by orography.

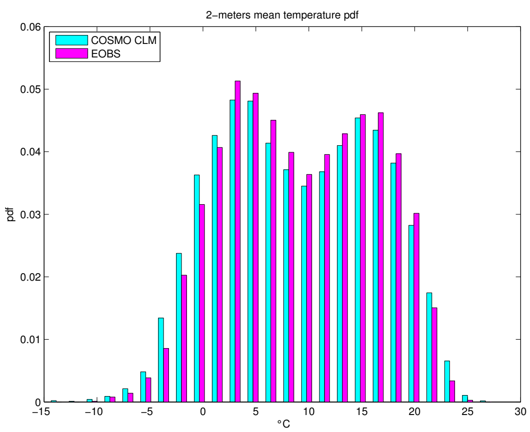

Figure 19:
2-meters mean temperature empirical probability distribution function of COSMO-CLM (cyan) and EOBS (magent).

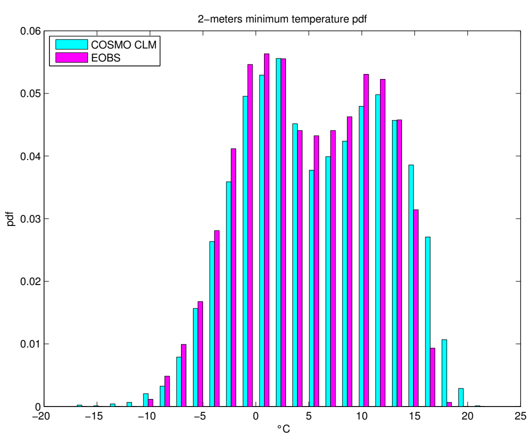

Figure 20:
2-meters minimum temperature empirical probability distribution function of COSMO-CLM (cyan) and EOBS (magent).

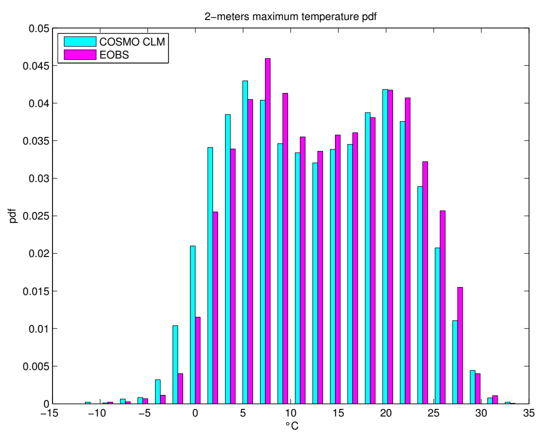

Figure 21:
2-meters maximum temperature empirical probability distribution function of COSMO-CLM (cyan) and EOBS (magent).

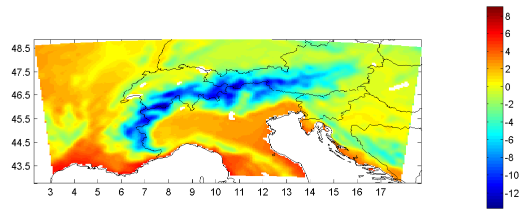

Figure 22:
10th percentile of 2-meters mean temperature (°C), from COSMO-CLM.

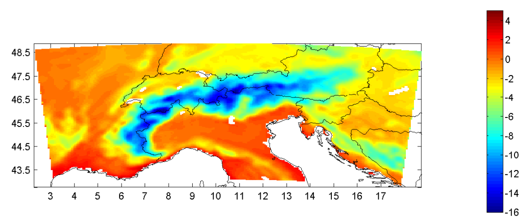

Figure 23:
10th percentile of 2-meters minimum temperature (°C), from COSMO-CLM.

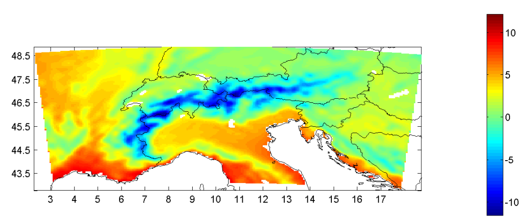

Figure 24:
10th percentile of 2-meters maximum temperature (°C), from COSMO-CLM.

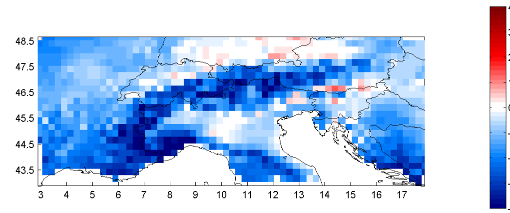

Figure 25:
Bias of 10th percentile of 2-meters mean temperature (°C) of COSMO-CLM in respect to EOBS data.

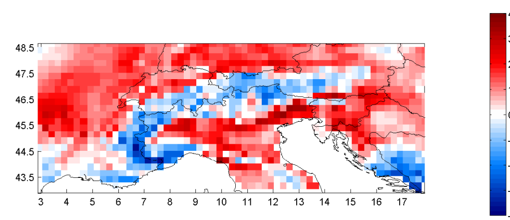

Figure 26:
Bias of 10th percentile of 2-meters minimum temperature (°C) of COSMO-CLM in respect to EOBS data.

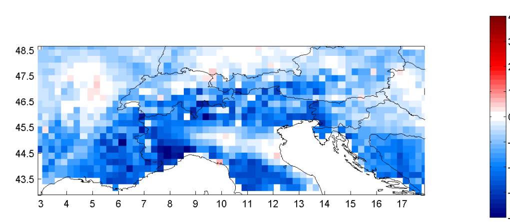

Figure 27:
Bias of 10th percentile of 2-meters maximum temperature (°C) of COSMO-CLM in respect to EOBS data.

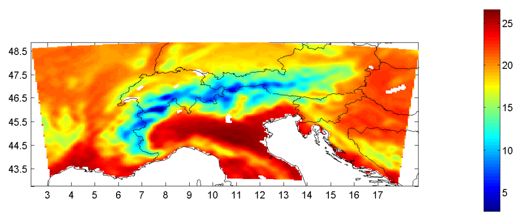

Figure 28:
90th percentile of 2-meters mean temperature (°C), from COSMO-CLM.

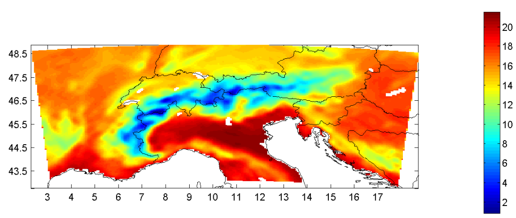

Figure 29:
90th percentile of 2-meters minimum temperature (°C), from COSMO-CLM.

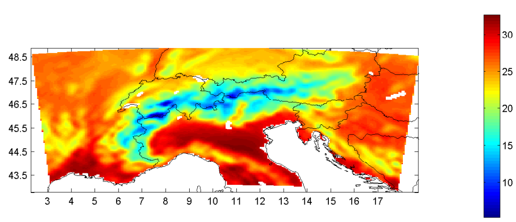

Figure 30:
90th percentile of 2-meters maximum temperature (°C), from COSMO-CLM.

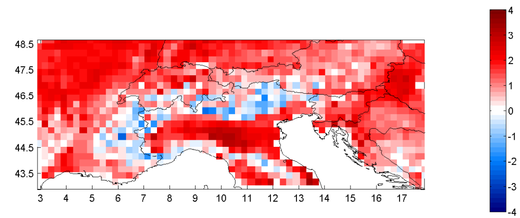

Figure 31:
Bias of 90th percentile of 2-meters mean temperature (°C) of COSMO-CLM in respect to EOBS data.

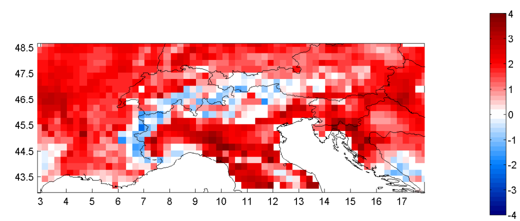

Figure 32:
Bias of 90th percentile of 2-meters minimum temperature (°C) of COSMO-CLM in respect to EOBS data.

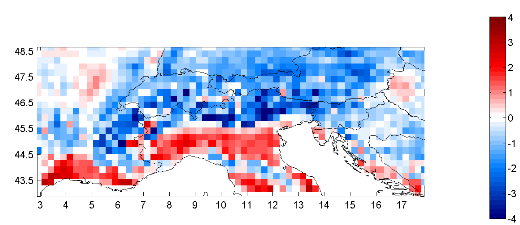

Figure 33:
Bias of 90th percentile of 2-meters maximum temperature (°C) of COSMO-CLM in respect to EOBS data.

3.2 - PRECIPITATION

The validation has been performed comparing the precipitation results with ETH dataset through seasonal means and statistical indices.

Analyzing the seasonal cycle, averaged over the whole domain (Figure 34), an overestimation occurs in spring, whereas there is an opposite trend in autumn. The percentage variation chart (Figure 35) highlights two peaks of bias in May $(+28\%)$ and October (-17%), while other months are chacterized by a very close match between model and observations.

Also the trend, averaged over the whole domain (Figure 36), is well represented, especially in the middle years of the simulations: a slight overestimation (max 1 mm/day) occurs in the first years and a very slight underestimation (max -0.33 mm/day) in the last ones.

An index analyzed is the average daily precipitation intensity (measured in mm) taken over values exceeding 1 mm/day, often referred as Simple Daily Intensity Index (SDII) (Figure 37).

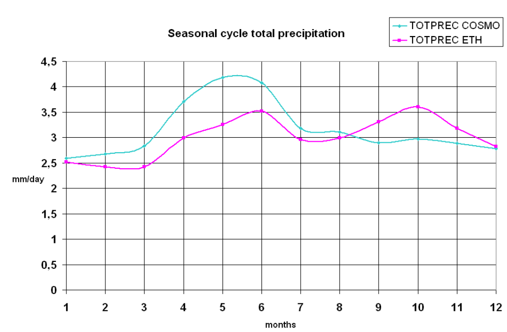

Figure 34:
Seasonal cycle of daily precipitation of COSMO-CLM (cyan) and ETH (magent).

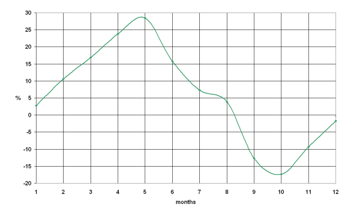

Figure 35:
Percentage variation of daily precipitation seasonal cycle of COSMO-CLM in respect to ETH.

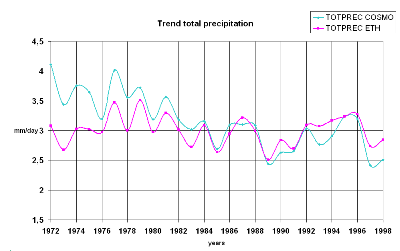

Figure 36:
Trend of daily precipitation of COSMO-CLM (cyan) and ETH (magent).

The model shows values hitting 15 mm/day in areas below Switzerland, near the boundaries between Italy and Slovenia, and in a small spot located east of Istria peninsula; compared with observations (Figure 40), they appear to be higher by 2-3 mm over most of the Alpine area, while tend to be smaller (down to -5 mm) in eastern zones.

Concerning the seasonal distribution of precipitations (Figures 38, 39, 43, 44) and their bias with respect to the observations (Figures 41, 42, 45, 46) there is an overestimation on the Alps, especially in spring. Differences of winter and summer values are, on average, between -1 and 2 mm/day in all the domain; in autumn, on the other hand, an underestimation (up to 4 mm/day) occurs in the Appennine and in the coast of Croatia.

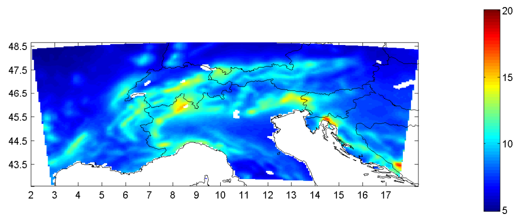

Figure 37:
Mean daily intensity (mm/day) of days with precipitation higher than 1 mm/day of COSMO-CLM.

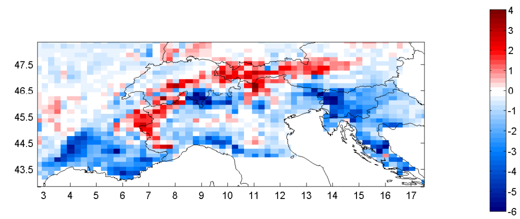

Figure 40:
Bias of mean daily intensity (mm/day) of days with precipitation higher than 1 mm/day of COSMO-CLM in respect to ETH data.

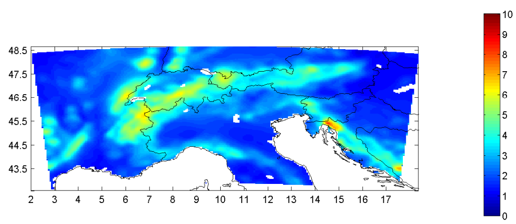

Figure 38:
Winter mean daily precipitation (mm/day) of COSMO-CLM.

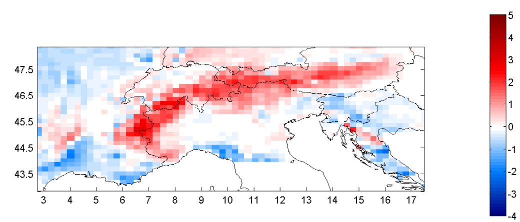

Figure 41:
Bias of winter mean daily precipitation (mm/day) of COSMO-CLM in respect to ETH data.

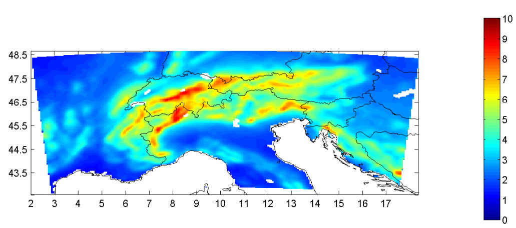

Figure 39:
Spring mean daily precipitation (mm/day) of COSMO-CLM.

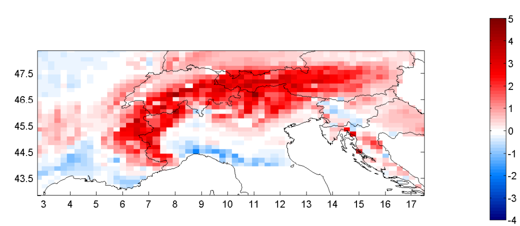

Figure 42:
Bias of spring mean daily precipitation (mm/day) of COSMO-CLM in respect to ETH data.

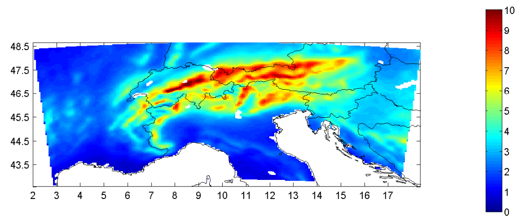

Figure 43:
Summer mean daily precipitation (mm/day) of COSMO-CLM.

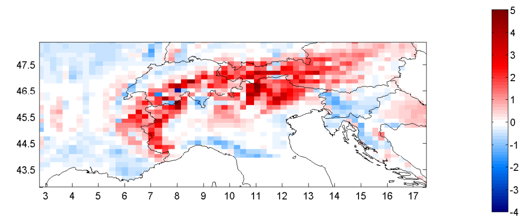

Figure 45:
Bias of summer mean daily precipitation (mm/day) of COSMO-CLM in respect to ETH data.

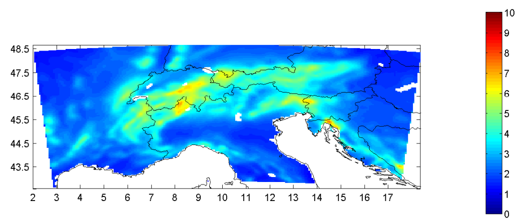

Figure 44:
Autumn mean daily precipitation (mm/day) of COSMO-CLM.

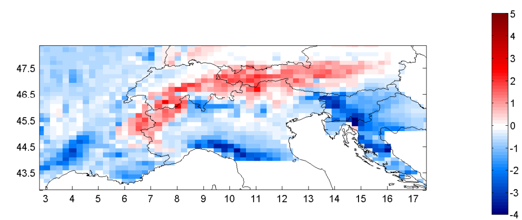

Figure 46:
Bias of autumn mean daily precipitation (mm/day) of COSMO-CLM in respect to ETH data.

In the density function (Figure 49), the most frequent events are those with daily precipitation lower than 2 mm/day. At these events, a slightly lower probability is attributed to COSMO-CLM in respect to ETH dataset. For precipitations higher than 2 mm/day, the regional model distribution is very well captured, with a general slight overestimation of COSMO-CLM data for intensities between 2 and 10 mm/day.

While examining percentile values of daily amounts (90th and 99th), a wider range of areas, including part of Switzerland and Austria, is interested by high values, although the most significant ones are collected in the zones mentioned for the SDII analysis: regarding 90th, they reach 14 mm/day, while 99ths are up to 25 mm/day.

In terms of differences from ETH, both 90th and 99th percentile values are higher by about 5 mm in almost the whole alpine area. In the southern regions, there is a good match between regional model and observations.

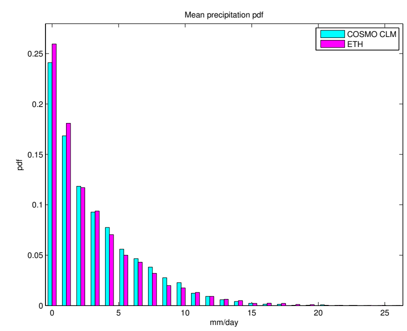

Figure 49:
Total precipitation empirical probability distribution function of COSMO-CLM (cyan) and ETH (magent).

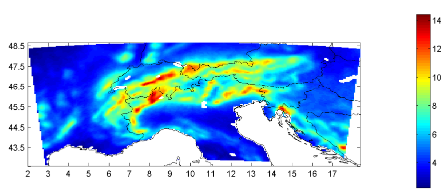

Figure 47:
90th percentile of daily precipitation (mm/day) of COSMO-CLM.

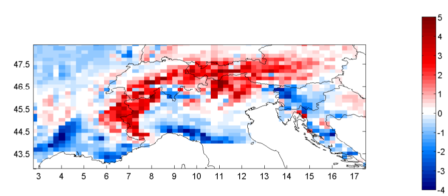

Figure 50:
Bias of 90th percentile of daily precipitation (mm/day) of COSMO-CLM in respect to ETH data.

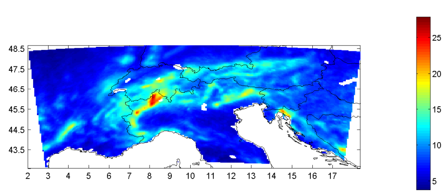

Figure 48:
99th percentile of daily precipitation (mm/day) of COSMO-CLM.

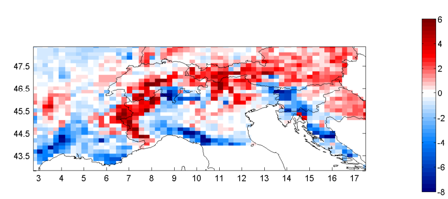

Figure 51:
Bias of 99th percentile of daily precipitation (mm/day) of COSMO-CLM in respect to ETH data.

For what concern extreme values, also the following indices have been also calculated:

1. Number of wet-days per year with precipitation between 1 mm/day and 20 mm/day representative for the class of weak precipitations;

2. Number of wet-days per year with precipitation between 20 mm/day and 60 mm/day representative for the class of moderate rains;

3. Number of wet-days per year with precipitation over 60 mm/day representative for the class of intense rains.

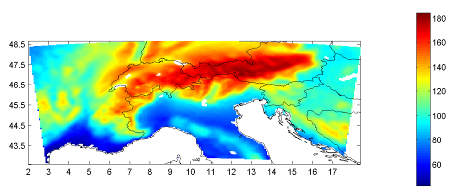

Figure 52:
Number of "weak precipitation days" (days/year), from COSMO-CLM.

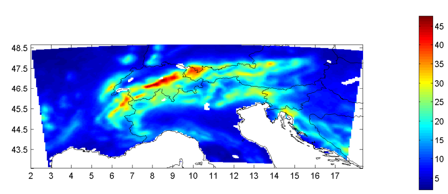

Figure 53:
Number of "moderate rain days" (days/year), from COSMO-CLM.

Such data have been taken as an average over the 27 years considered (1972-1998). Weak precipitation days interest all the Alps with a rate of about 170 days/year, especially east, but they turn to be 50-70 days more than real observations results; areas with a large amount of moderate rain days are reduced to a small area between Austria and Switzerland (45 days/year, about 20 more than ETH); finally, relevant peaks of intense rain days (7 days/year, a couple of days more than observations) are shown only in a few limited areas, which appear to be almost the same highlighted by SDII analysis.

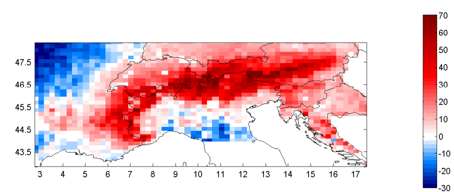

Figure 54:
Bias of "weak precipitation days" (days/year) of COSMO-CLM in respect to ETH data.

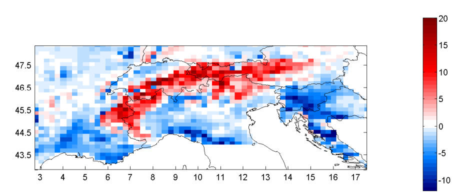

Figure 55:
Bias of "moderate rain days" (days/year) of COSMO-CLM in respect to ETH data.

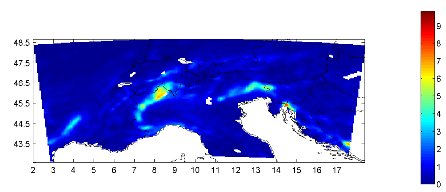

Figure 56:
Number of “intense rain days” (days/year), from COSMO-CLM.

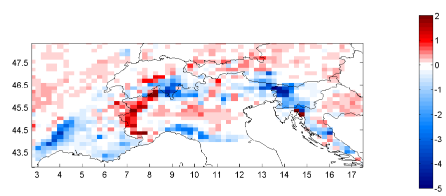

Figure 57:
Bias of “intense rain days” (days/year) of COSMO-CLM in respect to ETH data.

4 - CONCLUSIONS

Regional climate simulations over the Alpine area have been performed using the regional climate model COSMO-CLM at a spatial resolution of 8 km. The comparison between model and observed data shows that the mean 2 meter temperature is fairly well simulated over the Alpine region, where the bias never exceeds 3°C. In particular the full scale values are obtained during winter, with a cold bias in the Ligurian Alps, and during summer, with a hot bias in the Po Valley. For the other seasons and sub regions, the bias is mostly under 1°C. Concerning the precipitations, the model works reasonably well over the Alps with a bias always lower than 30%. In particular, two peaks of bias are evident in spring (with a maximum in May, $+28\%$) and autumn (with a maximum in October, -17%).

On the same area we have evaluated also the model capabilities in reproducing the probability density function of the temperature and precipitation and, therefore, some climatological extreme indices. This analysis of daily data of both 2 meter temperature and precipitation shows that the model captures fairly well the 2 meter temperature and precipitation distributions. Concerning 2 meter temperature, model and observations have two peaks in the same classes of the histogram. The mean 2 meter temperature distribution tails exhibit that the model is generally colder for the extremes classes. For the lower values (left tail) this is meanly due to a systematic error in the prediction of the maximum temperature while for the higher values (right tail) this is due to a systematic error in the minimum temperature. More specifically, the 10th and 90th percentile of the 2 meter temperature(mean, maximum and minimum) and their bias have been presented. Concerning the daily precipitation, different extremes values have been presented, such as 90th and 99th percentile. For both the indices the model exhibits a positive bias of about 5 mm in almost all the Alpine area, while in the southern region there is a good match with observations. In conclusion, the COSMO-CLM at the current resolution of 8 km allows a good representation of the 2 meter temperature and precipitation patterns. The latter statement suggests that the model resolution is fine enough to reproduce quite well the precipitation, while for temperature good results were obtained also using the resolution of 14 km. This suggests that simulations performed at 8 km resolution are capable of reproducing also the localized precipitation phenomena such as summer thunderstorm over the complex orography region of Alps.

Bibliography

[1] D. Bellafiore, E. Bucchignani, S. Gualdi, S. Carniel, V. Djurdjević, and G. Umgiesser. Assessment of meteorological climate models as inputs for coastal studies. *Ocean Dynamics*, 62(4):555–568, December 2011.

[2] A. Bellucci, S. Gualdi, E. Scoccimarro, and A. Navarra. NAO-ocean circulation interactions in a coupled general circulation model. *Climate Dynamics*, 31(7-8):759–777, April 2008.

[3] U. Böhm, M. Kücken, W. Ahrens, A. Block, D. Hauffe, K. Keuler, B. Rockel, and A. Will. CLM - The Climate Version of LM: Brief Description and Long-Term Applications. *Consortium for Small-Scale Modelling Newsletter No. 6*, (6), 2006.

[4] M. Brunetti, G. Lentini, M. Maugeri, T. Nanni, I. Auer, and B. Reinhard. Climate variability and change in the Greater Alpine Region over the last two centuries based on multi-variable analysis. 2225(February):2197–2225, 2009.

[5] E. Bucchignani, A. Sanna, S. Gualdi, S. Castellari, and P. Schiano. Simulation of the climate of the XX century in the Alpine space. *Natural Hazards*, 2011.

[6] S. Castellari. Climate Change, Impacts and Adaptation Strategies in the Alpine Space: Some Results from the INTERREG III B Project ClimChAlp. *Mountains as Early Indicators of Climate Change*, (April):17–18, 2008.

[7] J.H. Christensen, B. Hewitson, A. Busuioc, A. Chen, X. Gao, R. Held, R. Jones, R.K. Kolli, W.K. Kwon, R. Laprise, and Others. Regional climate projections. *Climate Change, 2007: The Physical Science Basis. Contribution of Working group I to the Fourth Assessment Report of the Intergovernmental Panel on Climate Change, University Press, Cambridge, Chapter 11*, pages 847–940, 2007.

[8] P. Faggian and F. Giorgi. An analysis of global model projections over Italy, with particular attention to the Italian Greater Alpine Region (GAR). *Climatic Change*, 96(1-2):239–258, July 2009.

[9] C. Frei and C. Schär. A Precipitation Climatology of the Alps from High-Resolution Rain-Gauge Observations. *International journal of climatology*, 900:873–900, 1998.

[10] M.R. Haylock, N. Hofstra, A.M.G. Klein Tank, E.J. Klok, P.D. Jones, and M. New. A European daily high-resolution gridded data set of surface temperature and precipitation for 1950-2006. *Journal of Geophysical Research*, 113(D20), October 2008.

[11] E.S. Im, E. Coppola, F. Giorgi, and X. Bi. Local effects of climate change over the Alpine region: A study with a high resolution regional climate model with a surrogate climate change scenario. *Geophysical Research Letters*, 37(5):1–6, March 2010.

[12] E.S. Im, E. Coppola, F. Giorgi, and X. Bi. Validation of a High-Resolution Regional Climate Model for the Alpine Region and Effects of a Subgrid-Scale Topography and Land Use Representation. *Journal of Climate*, 23(7):1854–1873, April 2010.

[13] B. Rockel and B. Geyer. The performance of the regional climate model CLM in different climate regions, based on the example of precipitation. *Meteorologische Zeitschrift*, 17(4):487–498, August 2008.

[14] B. Rockel, A. Will, and A. Hense. The Regional Climate Model COSMO-CLM (CCLM). *Meteorologische Zeitschrift*, 17(4):347–348, August 2008.

[15] C. Schär, D. Leuenberger, O. Fuhrer, D. Lüthi, and C. Girard. A New Terrain-Following Vertical Coordinate Formulation for Atmospheric Prediction Models. *M onthly weather review*, 130:2459—-2480, 2002.

[16] J. Steppeler, G. Doms, U. Schättler, H.W. Bitzer, A. Gassmann, U. Damrath, and G. Gregoric. Meso-gamma scale forecasts using the nonhydrostatic model LM. *Meteorology and Atmospheric Physics*, 82(1-4):75–96, January 2003.

[17] M. Suklitsch, A. Gobiet, A. Leuprecht, and C. Frei. High Resolution Sensitivity Studies with the Regional Climate Model CCLM in the Alpine Region. *Meteorologische Zeitschrift*, 17(4):467–476, August 2008.